

Electronic Supplementary Information

New zwitterionic radical salts: dimers in solution and unusual magnetic and luminescent properties in solid state

Guo-Ping Yong,* Chong-Fu Li, Ying-Zhou Li and Shi-Wei Luo

Department of Chemistry, University of Science and Technology of China, Hefei 230026, P.R. China

E-mail: gpyong@ustc.edu.cn.

Experimental procedures and measurements

1. Measurements

Microanalytical data (C, H, N) were collected on Vario ELIII elemental analyzer. Spectroscopic data were obtained using the following instruments: UV/Vis/NIR spectra from DUV-3700; FT-IR spectra (KBr disk, 4000–400 cm⁻¹) from Bruker EQUINOX55 FT-IR spectrophotometer; ¹H and ¹³C NMR spectra run on a Bruker Avance 400 MHz NMR spectrometer using dmso-*d*₆ as solvent. High-resolution mass spectra (HRMS) were recorded with an EI mode. Luminescence properties in DMSO solution were measured using RF-5301PC fluorescence spectrophotometer at room temperature. The photoluminescence quantum yields (PLQYs) were measured at room temperature in a 10⁻⁵ M DMF solution by comparing fluorescence intensities (integrated areas) of a standard sample (quinine sulfate, $\Phi = 0.54$)^{S1} and the unknown sample. The solid photoluminescence spectra were recorded at room temperature on a Fluorolog-3-TAU fluorescence spectrophotometer.

Electrochemical measurements were performed using computer-controlled LK98B II electrochemical analysis system with Pt-wire electrodes. All measurements were carried out at room temperature in DMSO solution (10⁻⁴ M) containing 0.1 M [n-Bu₄N][ClO₄] as supporting electrolyte, with scan rates of 50 mVs⁻¹ and reference to Hg₂Cl₂/Hg (SCE, 0.244 V at 298 K). Direct current conductivities were measured for the compaction pellets based on a standard four-probe technique attaching silver wires (0.26 mm Φ) on samples (hp 34401A). The EPR spectra were recorded on a JES-FA 200 ESR spectrometer at X-band. Temperature dependence of magnetic susceptibilities were measured for solid samples with a magnetic field of 1kOe using a SQUID magnetosusceptometer (Quantum Design MPMS) from 350 K to 2 K. Thermogravimetric analysis was performed under N₂ atmosphere with a heating rate of 10 °C min⁻¹ with a Shimadzu TGA-50H TG analyzer.

X-ray diffraction data for radicals **1** and **2** were collected at 291(2) K and 293(2) K on a Gemini S Ultra CCD diffractometer (Oxford diffraction Ltd.) equipped with Mo-K α monochromated radiation ($\lambda = 0.71073$ Å). Block crystals were glued to glass fibers with epoxy. The structure was solved by direct method (SHELXL 97) and completed by difference Fourier method (SHELXL 97). Refinement was performed against F^2 by weighted full-matrix least-squares (SHELXL 97),^{S2} and empirical absorption correction (SCALE3 ABSPACK) was

applied. All non-hydrogen atoms were refined with anisotropic displacement parameters. The C–H hydrogen atoms were placed in geometrically calculated positions; the N–H and O–H hydrogen atoms were located in the difference Fourier map and kept fixed in that position. Weighted *R* factor (R_w) and all goodness of fit S are based on F^2 , conventional *R* factor (*R*) is based on F .

2. Experimental procedures

All reagents were commercially available and used without further purification. $[Zn(bipo^-)Br]_n$ was synthesized following previously published procedure:^{S3} the mixture of hydrobromide salt of imidazo[1,2-*a*]pyridin-2(3H)-one (0.05 mol) and $Zn(NO_3)_2 \cdot 6H_2O$ (0.075 mol) was placed in a 75 cm³ Teflon-lined stainless autoclave containing DMF (15 mL) and H_2O (15 mL). The autoclave was sealed and heated at 130 °C for 30 h; red solid was obtained in a yield of 75 % (based on hydrobromide salt of imidazo[1,2-*a*] pyridin-2(3H)-one).

General procedure for the isolation of zwitterionic radical Hbipo⁻: Coordination polymer, $[Zn(bipo^-)Br]_n$, (15.65 g, 0.04 mol) was added to a solution of KOH (20.20 g, 0.36 mol) in 50 mL of H_2O , and the resulting mixture was vigorously stirred for 4 h, then EDTA (13.95 g, 0.047 mol) and 300 mL of H_2O were added, and continuously stirred for another 4 h. Thereafter, more H_2O was added, giving rise to a clear red solution. After filtered, the red filtrate was acidified with 37 % HCl to pH ≈ 6, leading to a yellow precipitate. After filtered again and washed with H_2O , yellow solid was soak overnight in saturated $NaHCO_3$ solution. The yellow solid then was filtered out and washed with H_2O ; recrystallization of yellow solid from DMF afforded yellow-green solid of Hbipo⁻. Yield: 7.45 g (0.03 mol, 74 %). Anal. (%) Calc. for $C_{14}H_{10}N_4O$: C, 67.19; H, 4.03; N, 22.39. Found: C, 67.06; H, 4.29; N, 22.14. **IR** (KBr, cm⁻¹): 3151m, 3071m, 1656s, 1615s, 1572s, 1543s, 1504m, 1458m, 1271m, 1022w, 887m, 748s, 735m, 657m. **¹H NMR** (400 MHz, dmso-*d*₆, 25 °C, ppm): 11.69 (broad, s, 1H, N(1)'H), 9.88 (d, *J* = 6.8 Hz, 1H, C(5)'H), 8.62 (d, *J* = 6.8Hz, 1H, C(8)'H), 8.30 (s, 1H, C(3)'H), 7.59 (d, *J* = 8.8 Hz, 1H, C(5)'H), 7.34~7.21(m, 3H, C(8)'H, C(7)'H, C(6)'H), 7.13 (dd, *J* = 6.8 Hz, 6.8Hz, 1H, C(7)'H), 6.90 (dd, *J* = 6.8 Hz, 6.4Hz, 1H, C(6)'H); **¹³C NMR** (75 MHz, dmso-*d*₆, 25 °C, ppm): 155.70, 143.62, 137.25, 135.67, 126.07, 125.05, 123.85, 123.48, 115.33, 113.41, 111.83, 111.53, 106.93, 96.67. **HRMS** (EI, m/z, [M]⁺): Calc. for $C_{14}H_{10}N_4O$: 250.0855, Found: 250.0847.

General procedure for the preparation of $[H(Hbipo^-)(ClO_4)]$ (**1**): Hbipo⁻ (0.2 g, 0.8 mmol) was added to 2.4 mL of aqueous $HClO_4$ (6 M), and the resulting mixture was heated at 53 °C till solid was completely dissolved, then filtered immediately. The filtrate was cooled, giving rise to solid. After filtered out, and soaked overnight using very diluent aqueous $HClO_4$, the resulting solid was again filtered and washed with H_2O to give yellow powder of **1**. Yield: 0.24 g (0.68 mmol, 85 %). Anal. (%) Calc. for $C_{14}H_{11}ClN_4O_5$: C, 47.95; H, 3.16; N, 15.98. Found: C, 47.52; H, 3.14; N, 15.96. **IR** (KBr, cm⁻¹): 3228s, 3165m, 1665vs, 1648vs, 1628vs, 1612vs, 1512m, 1465m, 1224w, 1175m, 1120s, 1112s, 1090vs, 770s, 748s, 622m. **¹H NMR** (400 MHz, dmso-*d*₆, 25 °C, ppm): 8.77 (d, *J* = 6.0 Hz, 1H, C(5)'H), 8.74 (d, *J* = 6.4 Hz, 1H, C(8)'H), 8.68 (s, 1H, C(3)'H), 7.97 (d, *J* = 8.8 Hz, 1H, C(5)'H), 7.78 (d, *J* = 7.6Hz, 1H, C(8)'H), 7.57 (dd, *J* = 7.6Hz, 8.0Hz, 1H, C(7)'H), 7.46~7.35 (m, 3H, C(6)'H, C(7)'H, C(6)'H); **¹³C NMR** (100 MHz, dmso-*d*₆, 25 °C, ppm): 156.23, 138.54, 135.05, 131.77, 128.19, 127.89, 127.24, 125.08, 117.01, 116.06, 111.88, 109.20, 104.57, 90.62. **HRMS** (EI, m/z, [M]⁺): Calc.

for C₁₄H₁₁N₄O: 251.0933, Found: 251.0899. Purple crystals of **1** suitable for X-ray diffraction analysis were obtained by slow diffusion of acetone into diluent aqueous HClO₄ of Hbipo⁻ at room temperature.

General procedure for the preparation of [H(Hbipo⁻)(ClO₄)][•](HClO₄•2H₂O) (**2**): Yellow powder of **1** (0.28 g, 0.8 mmol) was added to 7.2 mL of aqueous HClO₄ (1:1, v/v), and the resulting mixture was heated at 55 °C till yellow powder was completely dissolved. Pink crystals of **2** suitable for X-ray diffraction analysis were obtained by slow diffusion of ether into the above solution at 4 °C. Yield: 0.31 g (0.64 mmol, 80%). Anal. (%) Calc. for C₁₄H₁₂Cl₂N₄O₉ (C₁₄H₁₆Cl₂N₄O₁₁•2H₂O): C, 37.27; H, 2.68; N, 12.42. Found: C, 38.55; H, 2.96; N, 12.93. **IR** (KBr, cm⁻¹): 3125m, 1650s, 1612s, 1555m, 1530m, 1511m, 1460m, 1402m, 1243m, 1120vs, 1105vs, 1089vs, 1030s, 767m, 626m, 440w. **¹H NMR** (400 MHz, dmso-*d*₆, 25 °C, ppm): 8.76 (d, *J* = 6.8Hz, 1H, C(5)H), 8.72 (s, 1H, C(3)H), 8.63 (d, *J* = 6.8Hz, 1H, C(8)H), 8.02 (d, *J* = 8.8Hz, 1H, C(5)'H), 7.86 (d, *J* = 8.0Hz, 1H, C(8)'H), 7.62 (dd, *J* = 8.0Hz, 8.0Hz, 1H, C(7)H), 7.50~7.44 (m, 2H, C(6)'H, C(7)H), 7.39 (dd, *J* = 7.2Hz, 7.2Hz, 1H, C(6)H); **¹³C NMR** (100 MHz, dmso-*d*₆, 25 °C, ppm): 155.89, 138.56, 135.05, 131.99, 128.49, 127.97, 126.82, 125.17, 117.11, 116.18, 111.87, 109.29, 105.08, 90.68. **HRMS** (EI, m/z, [M-1]⁺): Calc. for C₁₄H₁₁N₄O: 250.0855, Found: 250.0851.

Computational methods: Geometry optimizations, and vibrational analyses when required, were performed at the spin-unrestricted (U)B3LYP/6-311++G(d, p) level of theory with Gaussian 03. The optimized structures were then used to calculate NMR parameters with the same functional but a basis set of 6-311+G (d, p). Chemical shifts δ were finally obtained as $\delta = \sigma_{\text{ref}} - \sigma_{\text{orb}}$, in which σ_{ref} is the reference shielding of ¹H in TMS (31.6544 ppm).

Calculated results (Table S1) indicate calculated ¹H NMR chemical shifts of paramagnetic radical monomers are obviously different from those of the observed dimers. However, when calculated only concerning diamagnetic molecules (non-radical), calculated ¹H NMR chemical shifts showed a fairly good agreement with experiments (diamagnetic dimers).

Table S1 Calculated and experimental ¹H chemical shifts (ppm) of Hbipo⁻ and H(Hbipo⁻).

H atom	Hbipo ⁻		Hbipo ⁻ ^a	H(Hbipo ⁻)		H(Hbipo ⁻) ^a
	δ_{calc}	δ_{exp}		δ_{calc}	δ_{exp}	
C(3)H	6.61	8.30	7.81	5.48	8.68	7.89
C(5)H	6.95	9.88	8.29	5.95	8.77	8.47
C(6)H	5.73	6.90	6.77	5.79	7.35	7.67
C(7)H	6.08	7.13	7.13	5.27	7.40	7.33
C(8)H	6.14	8.62	7.77	5.21	8.74	8.11
C(5)'H	5.47	7.59	7.38	5.75	7.97	7.78
C(6)'H	5.54	7.21	6.84	5.31	7.46	7.62
C(7)'H	3.74	7.28	6.90	5.46	7.57	7.86
C(8)'H	4.38	7.34	6.69	5.74	7.78	7.45
N(1)'H	4.99	11.69	10.95	6.51		7.97
N(1)H				9.97		13.54

^a Calculated only concerning diamagnetic molecules

References

- S1 K. Ye, J. Wang, H. Sun, Y. Liu, Z. Mu, F. Li, S. Jiang, J. Zhang, H. Zhang, Y. Wang and C.-M. Che, *J. Phys. Chem. B*, 2005, **109**, 8008.
 S2 G. M. Sheldrick, *SHELX-97, Programs for Crystal Structure Solution and Refinement*, University of Göttingen, Germany, 1997.
 S3 G. P. Yong, S. Qiao and Z.W. Wang, *Cryst. Growth Des.*, 2008, **8**, 1465.

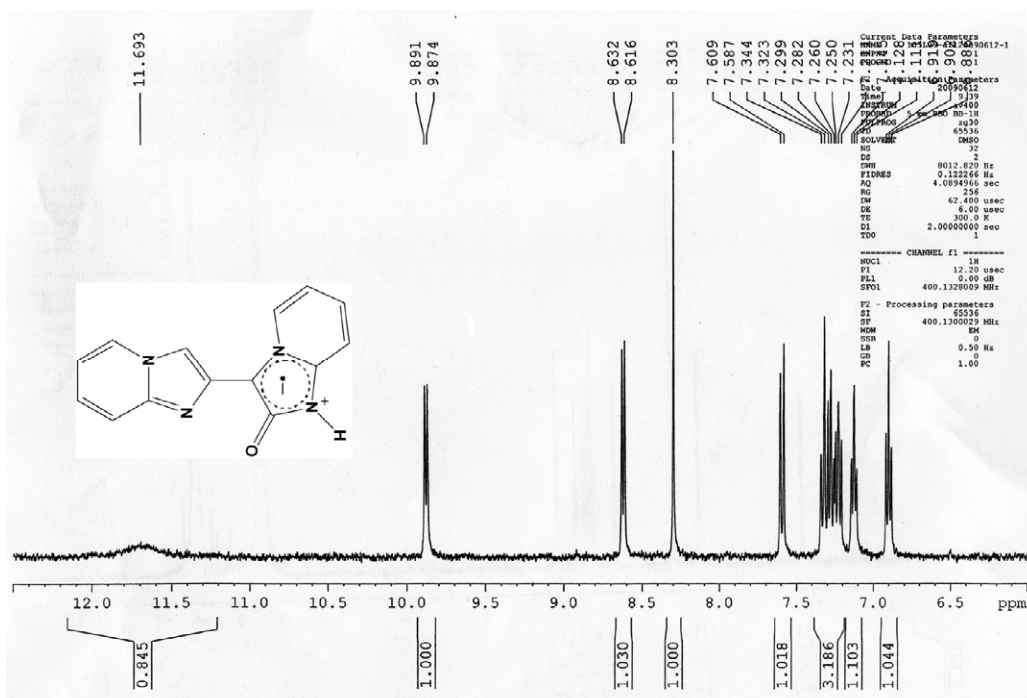


Fig. S1 ¹H NMR (400 MHz, dmso-*d*₆) for zwitterionic radical Hbipo⁻.

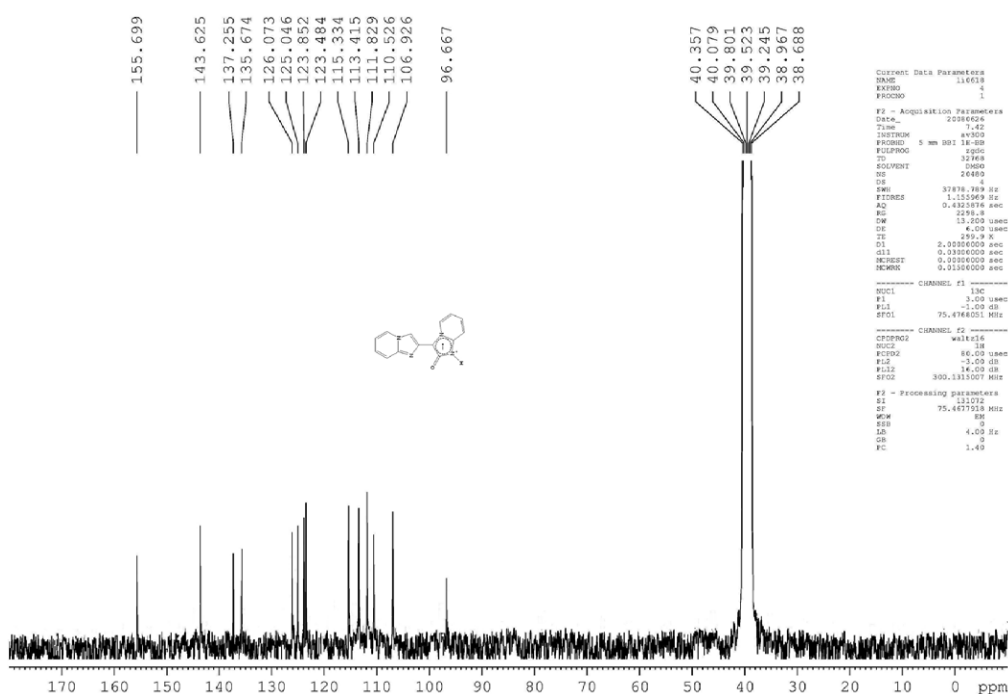


Fig. S2 ¹³C NMR (75 MHz, dmso-*d*₆) for zwitterionic radical Hbipo⁻.

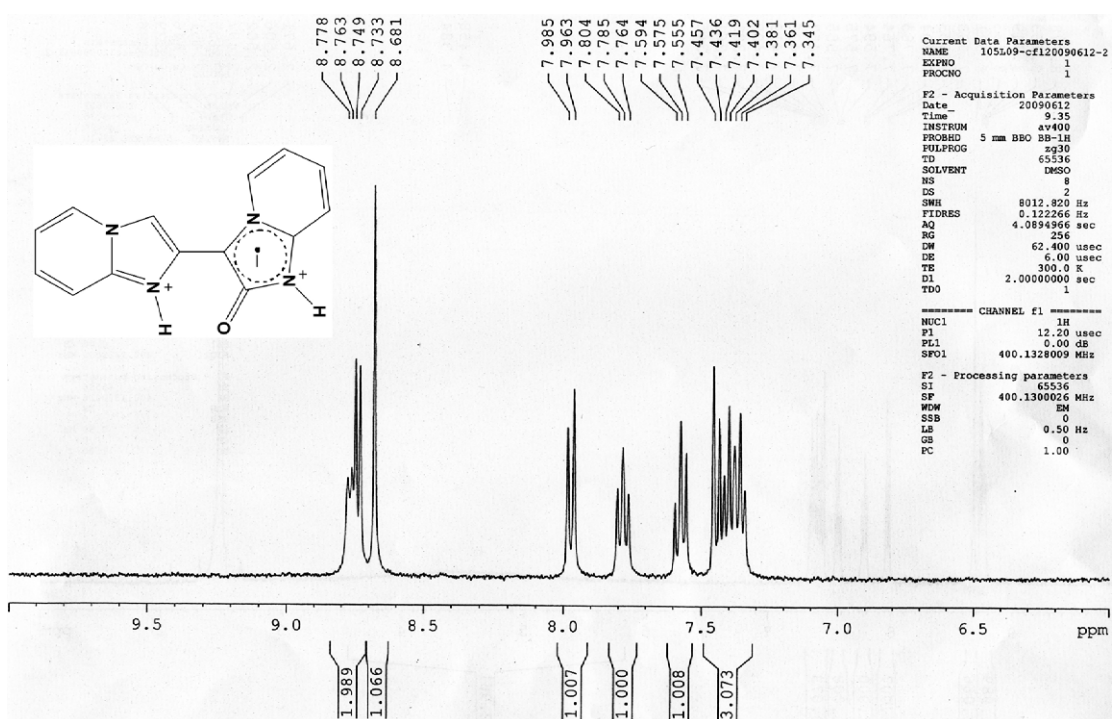


Fig. S3 ^1H NMR (400 MHz, dmso- d_6) for **1**.

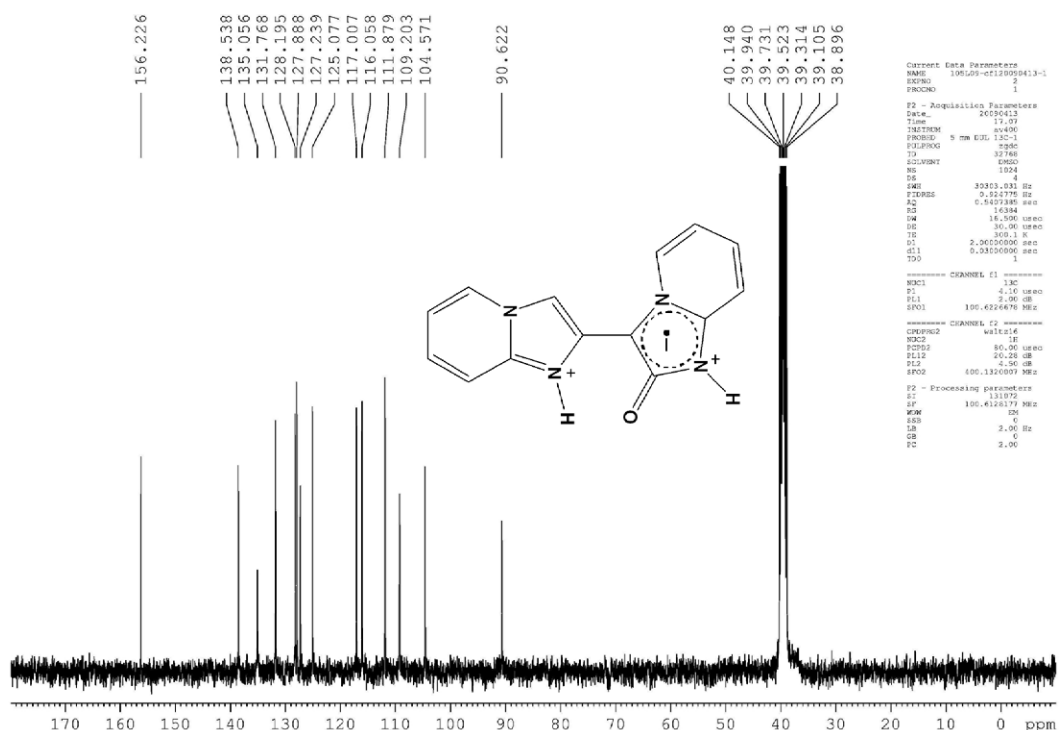


Fig. S4 ^{13}C NMR (100MHz, dmso- d_6) for **1**.

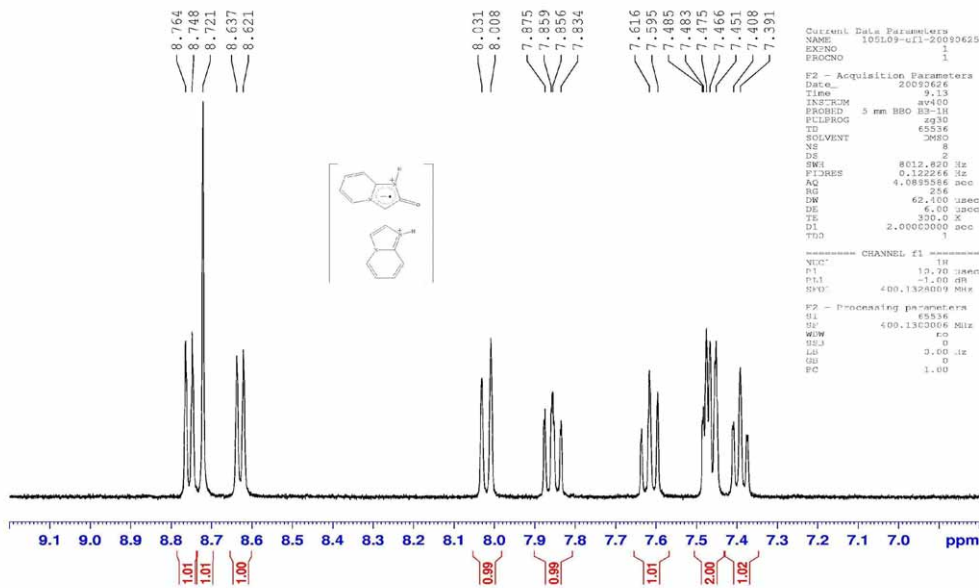


Fig. S5 ^1H NMR (400 MHz, dmso- d_6) for **2**.

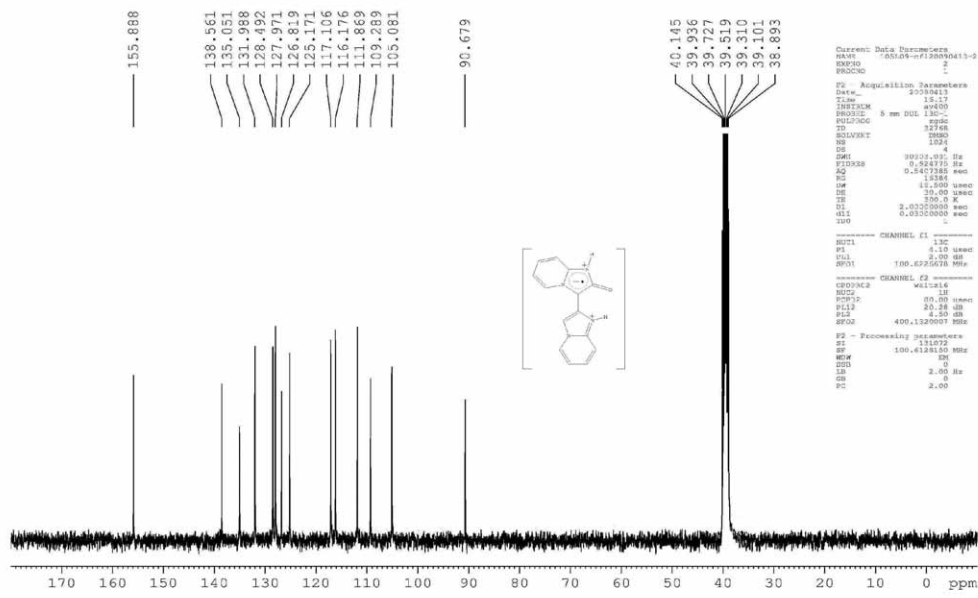


Fig. S6 ^{13}C NMR (100 MHz, dmso- d_6) for **2**.

Photophysical and electrochemical properties of three radicals in solution at room temperature

Table S2 Photophysical and electrochemical properties of radicals at room temperature.

Radical	Abs. λ_{abs} (nm) ^a	Solution PL λ_{em} (nm) ^b	Solid PL λ_{em} (nm) ^c	PLQYs ^d	CV E _{1/2} (V) ^e
Hbipo ⁻	262,302,367, 421; 491,533,579,705	465	523,630	0.034	0.55,0.67; -0.14
1	264,303,386, 412; 573,616	470	462,598	0.058	0.56,0.71; -0.30
2	261,302,368, 420; 528,568,616,703	461	431,587	0.041	0.53,0.72; -0.12

^a In 10⁻⁶ M DMSO solution for wavelength range between 250 to 465 nm; in 10⁻³ M DMSO solution for wavelength range between 465 to 1200 nm. ^b In 10⁻⁵ M DMSO solution, excitation wavelength for the emission measurements was 278 nm for Hbipo⁻, 306 nm for **1** and 419 nm for **2**, respectively. ^c Excitation wavelength for the emission measurements of three radicals was 366 nm. ^d PLQYs were measured in a 10⁻⁵ M DMF solution using quinine sulfate ($\Phi = 0.54$) as a reference. Corrections were made due to the change in solvent refractive indices. ^e In 10⁻⁴ M DMSO solution containing 0.1 M *n*-Bu₄NClO₄ vs SCE.

To obtain further information on the electronic structure of these radicals, the UV-Vis spectra were recorded in 10⁻⁶ M DMSO solution (Fig. S7). The absorption spectra show broad bands from 255 to 465 nm, and the most intense bands are at *ca.* 263 nm and moderately intense bands are at longer wavelengths which extend to the visible region. The bands between 250 and 300 nm can be assigned to spin-allowed singlet transitions. The absorption bands around 400 nm can probably be attributed to the intense spin-allowed $\pi-\pi^*$ transitions localized on the imidazo[1,2-*a*]pyridine units.

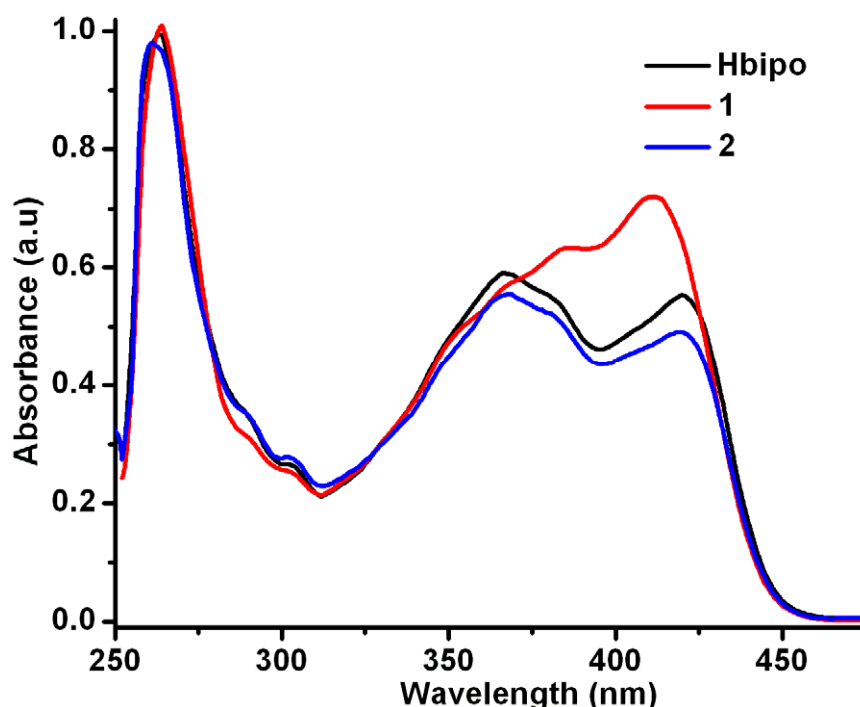


Fig. S7 UV-Vis absorption spectra of three radicals in DMSO solution.

In DMSO solution, the electrochemical behaviors of three zwitterionic radicals were investigated by cyclic voltammetries, which exhibit similar quasi-reversible oxidation processes and irreversible reduction process (Fig. S8). Fig.S9 shows the similar photoluminescence (PL) spectra of three radicals obtained from deaerated DMSO solution at room temperature, with the maximum emission bands near 465 nm.

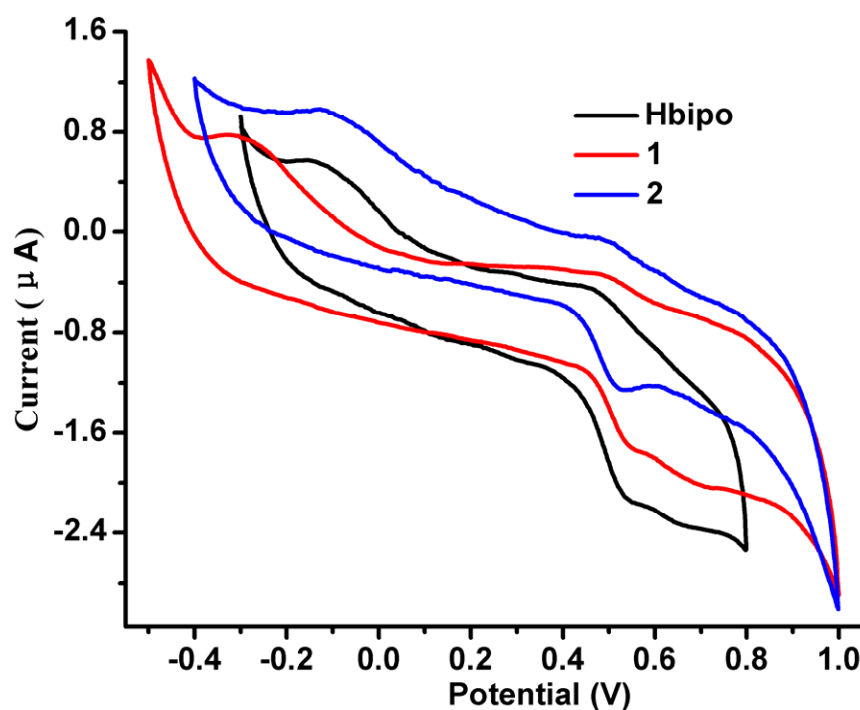


Fig. S8 Cyclic voltammetries of three radicals in DMSO solution.

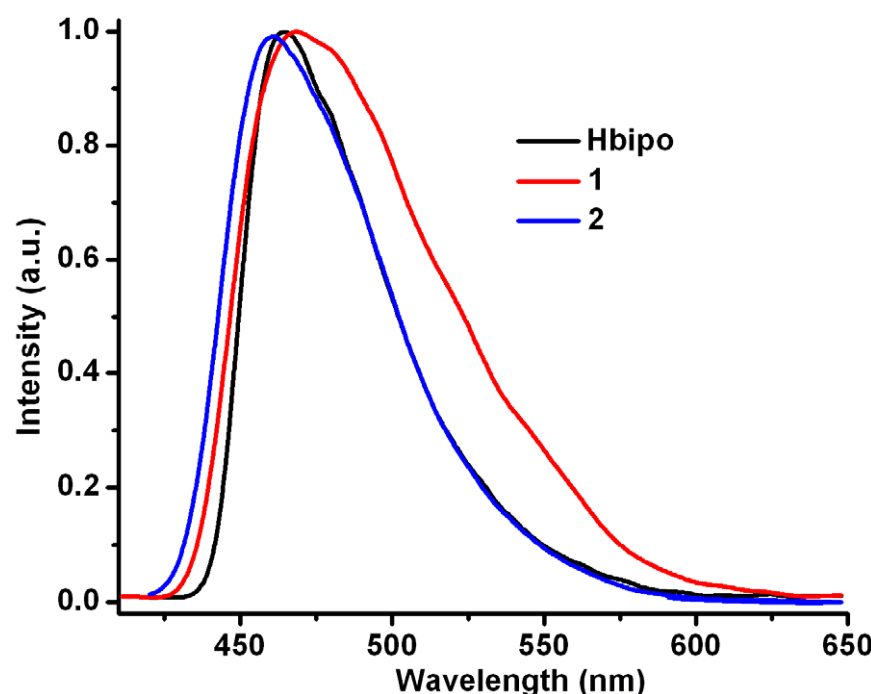


Fig. S9 Photoluminescence spectra of three radicals in DMSO solution.

Structural diagrams

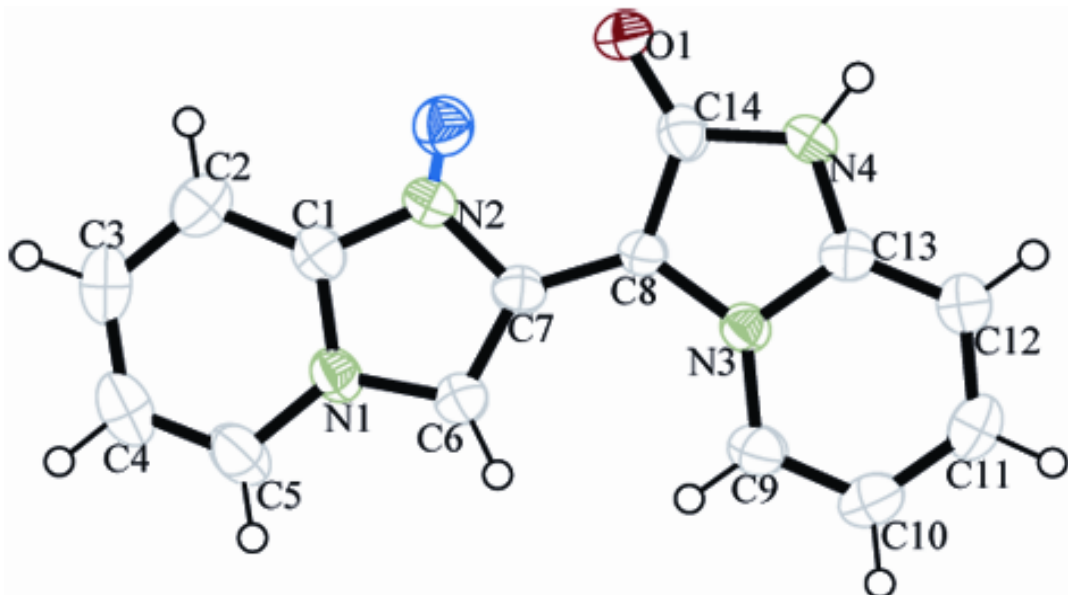


Fig. S10 ORTEP diagram of $[H(Hbipo^{\cdot})]^+$ cation in **1** and **2** with ellipsoids drawn at 50% probability.

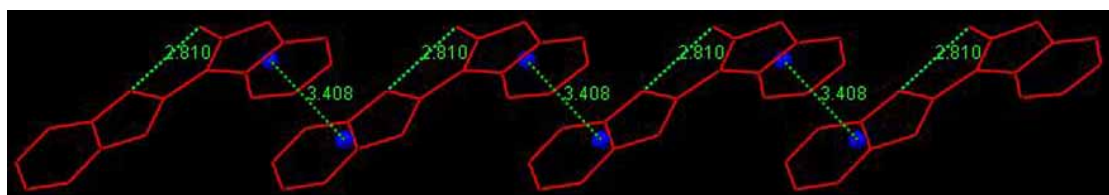


Fig. S11 The slipped π -stacking 1D chain of **1**, showing intramolecular hydrogen-bonds and intermolecular π - π separation distances.

It is notable that in **2**, one guest water molecule (O_{11}) forms two hydrogen bonds with oxygen atom of $[H(Hbipo^{\cdot})]^+$ moiety ($O_{11}\cdots O_1 = 2.489(4)$ Å) and one of oxygen atoms in $HClO_4$ molecule ($O_{11}\cdots O_5 = 2.894(5)$ Å), respectively. As shown in Fig.S12, the slipped π -stacking chains are further linked into two-dimensional supramolecular network in the *bc* plane through hydrogen bonding interactions with $N_2\cdots O_9$ (one of oxygen atoms in ClO_4^- anion) of $2.888(4)$ Å, $O_7\cdots O_{10}$ (another guest water molecule) of $2.962(5)$ Å and $O_{10}\cdots N_{4^i}$ (*i*: $-x, y, -z+1/2$) of $2.756(5)$ Å. Interestingly, two water molecules (O_{10} and O_{11}) serve as bridging hydrogen-bonding action.

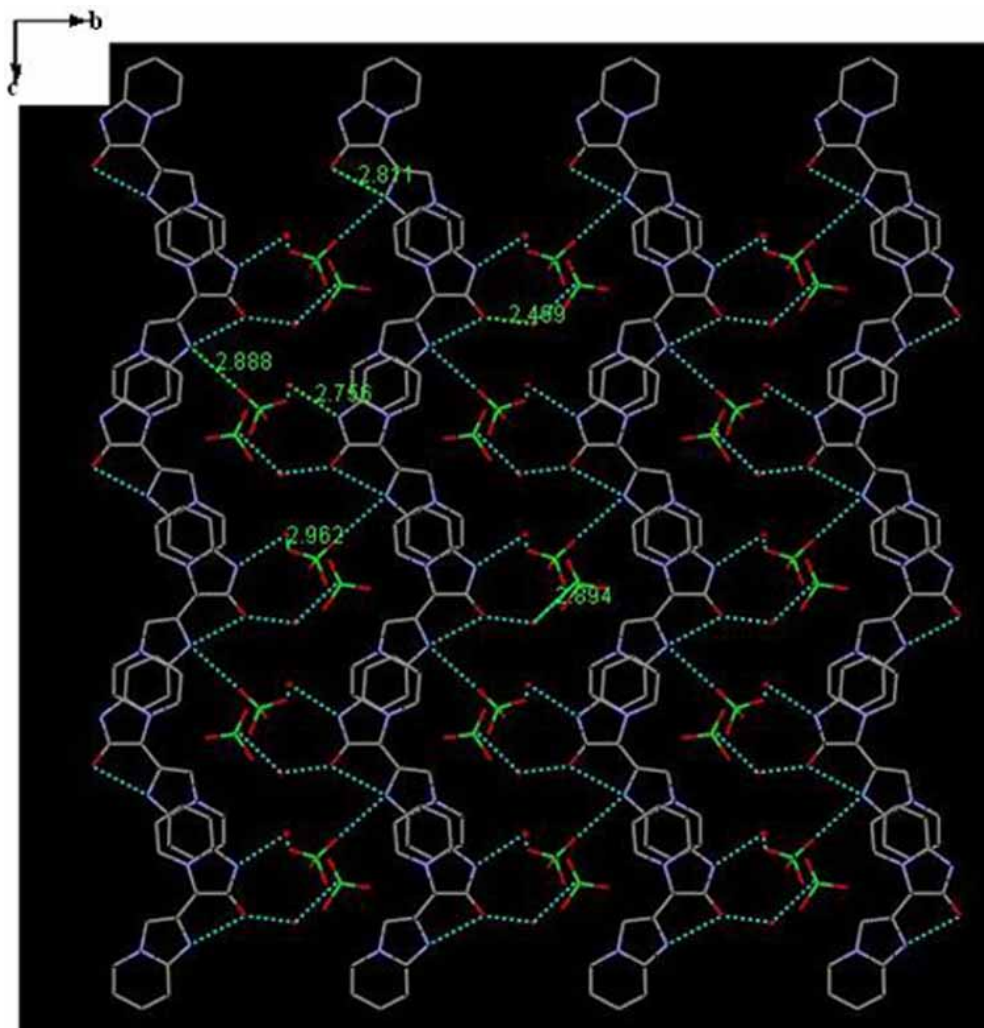


Fig. S12 Two-dimensional supramolecular network in **2** as viewed down the *a*-axis, the dotted lines represent hydrogen bonds.

The X-band EPR spectra and magnetic properties

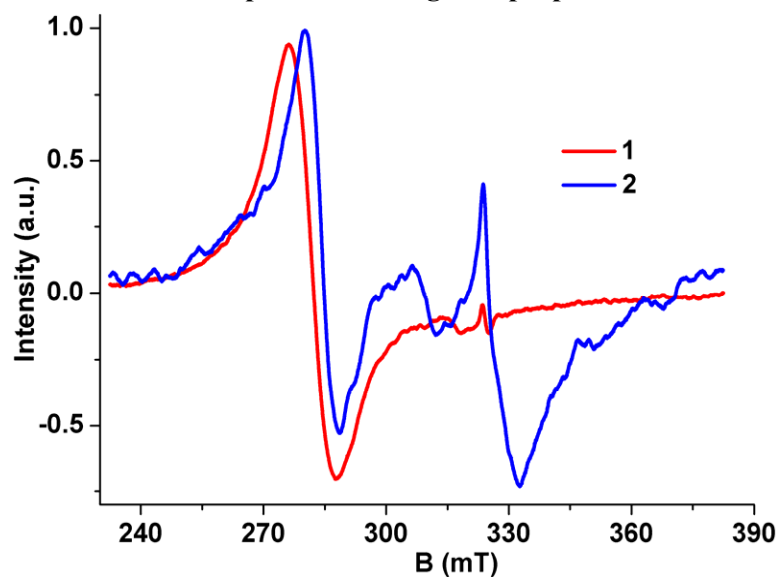


Fig. S13 Crystalline EPR spectra of **1** and **2** at room temperature.

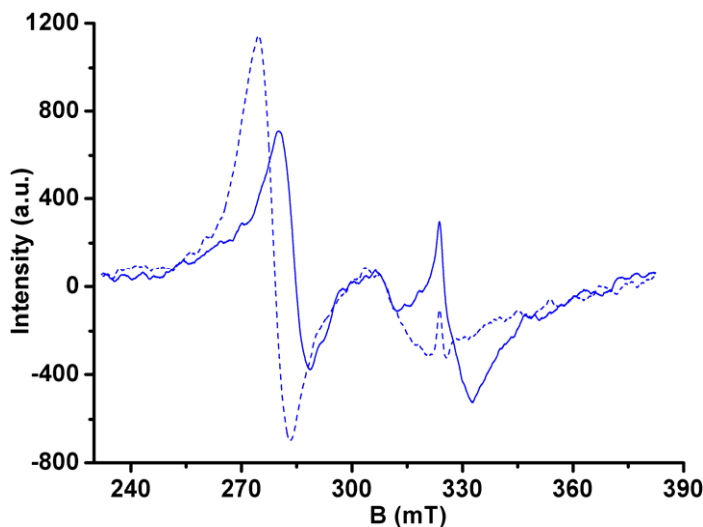


Fig. S14 Crystalline EPR spectra of **2** at room temperature with different magnetic field orientation (dashed line corresponding to EPR signal after rotating crystalline about 90° when the magnetic field direction was fixed).

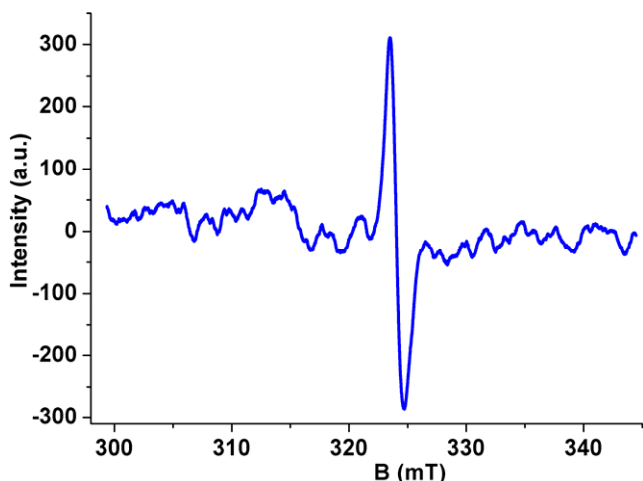


Fig. S15 Isotropic EPR signal at room temperature for uniform powder of **2** after grinding.

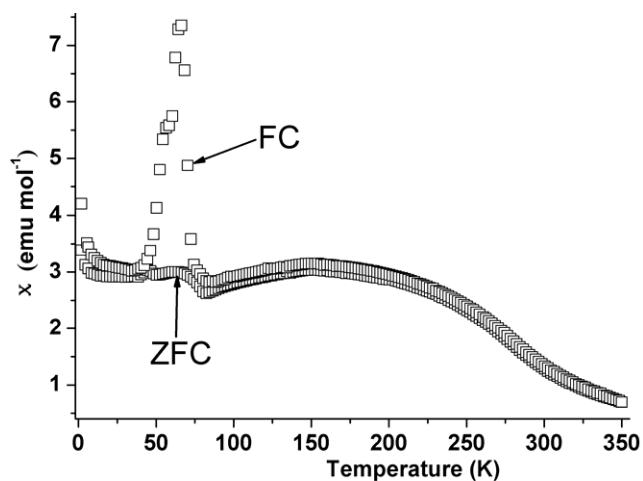


Fig. S16 Plots of FC/ZFC susceptibilities versus temperature of **1**.

Thermogravimetric analysis (TGA) of **2** was performed in N₂ at a heating rate of 10 °C min⁻¹ on polycrystalline sample. The TG curve of **2** displays the slow weight loss starts at *ca.* 70 °C and ends at *ca.* 138 °C (7.0%), corresponding to the loss of two guest water molecules (Calc. 7.4 %), and then abrupt weight loss (91.2 %) between 270 and 286 °C, corresponding to the loss or decomposition of two HClO₄ molecules and Hbipo moiety (Calc. 92.6 %), as shown in Fig.S17.

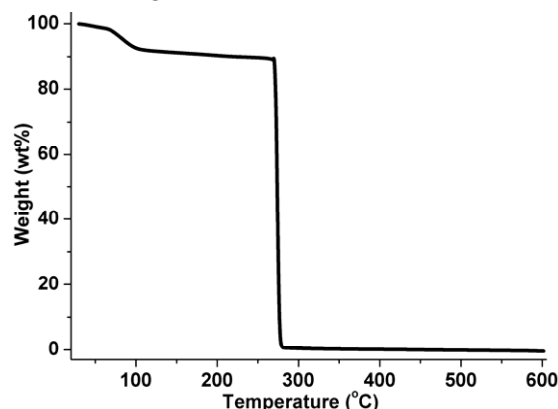


Fig. S17 TGA curve of **2**.

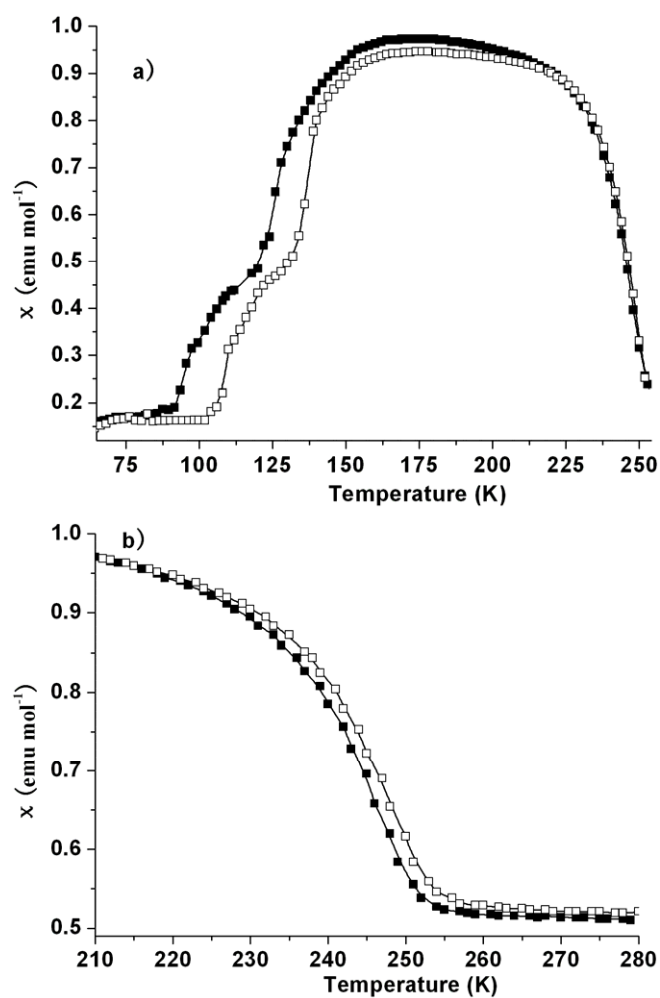


Fig. S18 Temperature dependence of susceptibility for **1** (a) and **2** (b) upon cooling (closed squares) and upon heating (open squares).

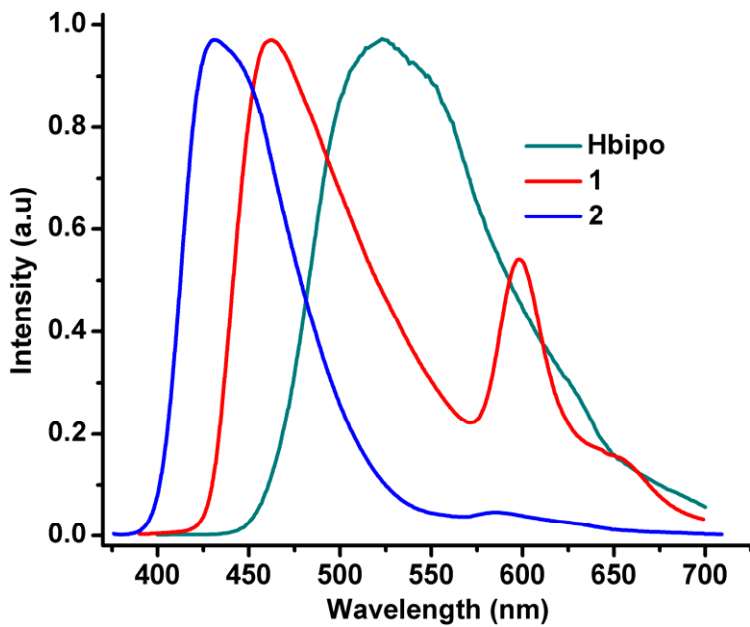


Fig. S19 Solid photoluminescence spectra of three radicals.

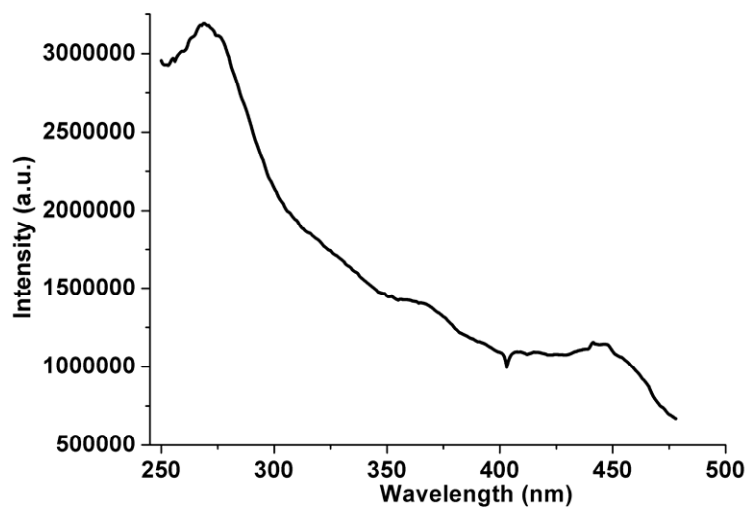


Fig. S20 Solid excitation spectrum of 1.